Molecular Therapy
Nucleic Acids
Original Article

Antisense Oligonucleotides Promote Exon Inclusion and Correct the Common c.-32-13T>G *GAA* Splicing Variant in Pompe Disease

Erik van der Wal,[1,2,3,4] Atze J. Bergsma,[1,2,3,4] Joon M. Pijnenburg,[1,2,3] Ans T. van der Ploeg,[2,3] and W.W.M. Pim Pijnappel[1,2,3]

[1]Molecular Stem Cell Biology, Department of Clinical Genetics, Erasmus Medical Center, 3015 CN Rotterdam, the Netherlands; [2]Department of Pediatrics, Erasmus Medical Center, 3015 CN Rotterdam, the Netherlands; [3]Center for Lysosomal and Metabolic Diseases, Erasmus Medical Center, 3015 CN Rotterdam, the Netherlands

The most common variant causing Pompe disease is c.-32-13T>G (IVS1) in the acid α-glucosidase (*GAA*) gene, which weakens the splice acceptor of *GAA* exon 2 and induces partial and complete exon 2 skipping. It also allows a low level of leaky wild-type splicing, leading to a childhood/adult phenotype. We hypothesized that *cis*-acting splicing motifs may exist that could be blocked using antisense oligonucleotides (AONs) to promote exon inclusion. To test this, a screen was performed in patient-derived primary fibroblasts using a tiling array of *U7* small nuclear RNA (snRNA)-based AONs. This resulted in the identification of a splicing regulatory element in *GAA* intron 1. We designed phosphorodiamidate morpholino oligomer-based AONs to this element, and these promoted exon 2 inclusion and enhanced GAA enzyme activity to levels above the disease threshold. These results indicate that the common IVS1 *GAA* splicing variant in Pompe disease is subject to negative regulation, and inhibition of a splicing regulatory element using AONs is able to restore canonical *GAA* splicing and endogenous GAA enzyme activity.

INTRODUCTION

Pre-mRNA splicing is a highly regulated process, the outcome of which is critical for homeostasis and disease. The diversity of splicing variants positively correlates with evolutionary complexity, as it allows for an expansion of the possible protein isoforms that are derived from the same genetic information.[1] The regulation of splicing is still relatively poorly understood, which is caused by the many factors that can affect splicing outcome. At the level of RNA sequences, splicing regulatory elements are loosely defined. The splice site junctions, as well as the polypyrimidine (pY) tract and branch point, are relatively easy to identify. Splice regulatory elements exist, including the exonic and intronic splice enhancer and silencer elements (ESEs, ESSs, ISEs, and ISSs, respectively), but these are more difficult to predict.[2] The expression levels of splicing regulatory proteins can also play an important role in splicing outcome.[3] Furthermore, the speed of RNA polymerase II transcription is thought to affect splicing efficiency, because splicing mainly occurs co-transcriptionally, and the available splice sites that are present in the protruding pre-mRNA within a certain time frame compete for the splicing machinery.[4,5] Additional levels of regulation are chromatin modifications and the composition of the UTRs.[6,7] All together, these diverse levels of regulation highlight the requirement for experimental testing of alternative splicing to validate predictions.

Disruption of splicing has been documented in a large number of human disorders. Approximately 9% of pathogenic variants annotated in the Human Gene Mutation Database are linked to splicing defects (http://www.hgmd.cf.ac.uk/). In this database, variants that affect splicing predominantly concern those that are located at splice site junctions.[8] This is caused by the inherent detection bias for these variants, which are mostly identified using splice prediction algorithms. However, variants can also alter splicing by the generation of new splice sites[9,10] or by disturbing or generating other splice regulatory elements.[11,12] In addition, variants in the coding region can have more than one effect (i.e., a missense variant can also have an effect on splicing).[9] Furthermore, indirect effects on target genes are known (e.g., in response to mutations in master splicing factors such as the muscleblind family, SF3B1, and U2AF35).[13,14] The consequences of such events can be diverse and may include (partial) exon skipping and/or (partial) intron retention. The final mRNA may be in frame, which in certain cases may result in a protein product that retains some biological activity. A reading frameshift usually results in mRNA decay and absence of a protein product, although the extent at which decay occurs may vary. It is likely that many more pathogenic splicing variants exist that are located outside the region of canonical splice sites, and that the percentage of identified variants that affect splicing will increase in the future.

Received 29 October 2016; accepted 3 March 2017;
http://dx.doi.org/10.1016/j.omtn.2017.03.001.

[4]These authors contributed equally to this work.

Correspondence: W.W.M. Pim Pijnappel, Departments of Clinical Genetics and Pediatrics, Erasmus Medical Center, 3015 CN Rotterdam, the Netherlands.
E-mail: w.pijnappel@erasmusmc.nl

Antisense oligonucleotides (AONs) can modulate splicing by binding to the pre-mRNA and blocking splicing regulatory sequences. One type of AON has been modified from the naturally occurring *U7* small nuclear RNA (snRNA), which is normally utilized in histone pre-mRNA processing but has been modified to target the pre-mRNA of choice.[15] *U7* snRNA-based AONs are stabilized by a stem loop and also contain an antisense sequence that is used for targeting.[16] Another strategy is the use of chemically modified AONs that are capable to bind to RNA via Watson-Crick base pairing but are insensitive to RNase-mediated degradation due to their modified backbone chemistry. Various backbones with different properties are known, which include phosphorodiamidate morpholino oligomer (PMO), 2′-O-methyl phosphorothioate, 2-O-methoxyethyl phosphorothioate, and tricyclo-DNA modifications.[17]

A straightforward approach to modulate splicing using AONs is to block a splice junction. This will result in exon skipping, which can be advantageous, for example, to bypass a mutation hotspot and to restore the reading frame. This will only work when the resulting truncated protein is at least partially active, which is the case for the dystrophin protein, providing a potential therapy for Duchenne muscular dystrophy.[18,19] This approach has been tested in multiple clinical trials and has moved forward toward conditional approval by the US Food and Drug Administration (FDA).[20] Many other examples have been published, in which a cryptic splice site is blocked with an AON to restore canonical splicing (reviewed in Havens and Hastings[17]). We recently showed that this is possible in the case of *GAA* variants that cause Pompe disease.[9] Restoration of splicing becomes more challenging in cases where a splicing variant causes exon skipping and requires promotion of exon inclusion. When there is no clear cryptic splice site involved that can be blocked by an AON, such cases require the identification of ISS or ESS elements that are critical for exon inclusion. Blocking of these splice silencers with an AON may in turn promote exon inclusion. Few examples for promotion of exon inclusion exist; notably, for spinal muscular atrophy, caused by variants in the *SMN1* gene, AONs have been designed that reactivate the normally silent sister gene *SMN2*. *SMN2* contains an exonic variant that causes exon skipping, and AONs have been identified that block ESS or ISS sequences and promote exon inclusion.[21,22] One of these, which targets the ISS, is currently being tested in clinical trials.[23]

Because AONs are sequence specific, they are usually only suitable for a subgroup of patients with similar gene variants. In Pompe disease, a common splicing variant occurs in the majority of Caucasian patients with the childhood/adult form. This well-described variant, c.-32-13T>G (also known as IVS1, or r.-32-13u>g at the RNA level), is located in the pY tract of exon 2 of the acid α-glucosidase (*GAA*) pre-mRNA and causes weakening of the splice acceptor site, resulting in complete or partial skipping of exon 2.[24–27] This exon contains the translation start codon, and its skipping results in mRNA degradation and a subsequent reduction of GAA protein production. Approximately 10%–15% of transcripts are spliced normally and produce a low level of wild-type GAA protein, which explains why these patients develop the childhood/adult form of Pompe disease. A minimum GAA activity of 20% of the average healthy control values is required to prevent the disease.[28] The restoration of splicing from the IVS1 variant using AONs would potentially provide a therapeutic option for the majority of Caucasian patients with Pompe disease. This may be beneficial in addition to or instead of the current enzyme replacement therapy, which has a partial and heterogeneous response and is extremely expensive. However, splicing correction from the IVS1 variant requires promotion of exon inclusion, and no negatively acting splicing regulatory sequences in the *GAA* gene that are amenable to inhibition using AONs are currently known.

Here, we used a screen to modulate endogenous *GAA* splicing using *U7* snRNA-based AONs expressed via lentiviral transduction in patient-derived primary fibroblasts. This resulted in the identification of *cis*-acting splicing regulatory elements that were subsequently tested using PMO-based AONs. Two overlapping AONs were identified that promoted inclusion of exon 2 in cells from patients carrying the IVS1 variant. In cells from healthy controls, the AONs did not change *GAA* splicing or expression, confirming that they acted on splicing rather than elevating total *GAA* transcript levels. The AONs increased GAA enzymatic activity in patient-derived cells to above the disease threshold of 20%. These findings demonstrate the feasibility to correct aberrant splicing from the common IVS1 *GAA* variant by blocking a negative splicing element to promote exon inclusion.

RESULTS

Aberrant Splicing of *GAA* Pre-mRNA in the Presence of the IVS1 Variant

Previous work resulted in the characterization of aberrant splicing caused by the IVS1 *GAA* variant.[24–27] Splicing products include wild-type *GAA* mRNA (N) caused by leaky normal splicing, partial skipping of exon 2 caused by utilization of a cryptic splice site in exon 2 (SV3), and full skipping of exon 2 (SV2). These products can be identified by flanking exon RT-PCR in primary fibroblasts using primers that anneal to exons 1 and 3 (Figure 1A). Splicing is subject to regulation by additional *cis*-acting RNA sequences besides the sequences surrounding the canonical splice sites. These include ESSs, ISSs, ESEs, and ISEs and can be located distant from canonical splice sites (hypothetical example given in Figure 1B). Approximately 10%–15% of the *GAA* pre-mRNA is correctly spliced, indicating that the pathogenic effect of the IVS1 variant is not fully detrimental to splicing of *GAA* exon 2. We hypothesized that it may be possible to promote exon 2 inclusion by inhibition of a splicing negatively acting splicing regulatory element using an AON. To test this, in silico prediction was performed using several algorithms, which resulted in a plethora of splicing regulatory elements (Figure 1C). However, the results were algorithm dependent and many predicted enhancer and silencer sequences overlapped without indicating an obvious candidate silencer element that could be amenable to inhibition by an AON.

Identification of Repressors of *GAA* Exon 2 Inclusion

To identify splicing regulatory elements experimentally, an unbiased screen was performed using a non-overlapping tiling array of AONs

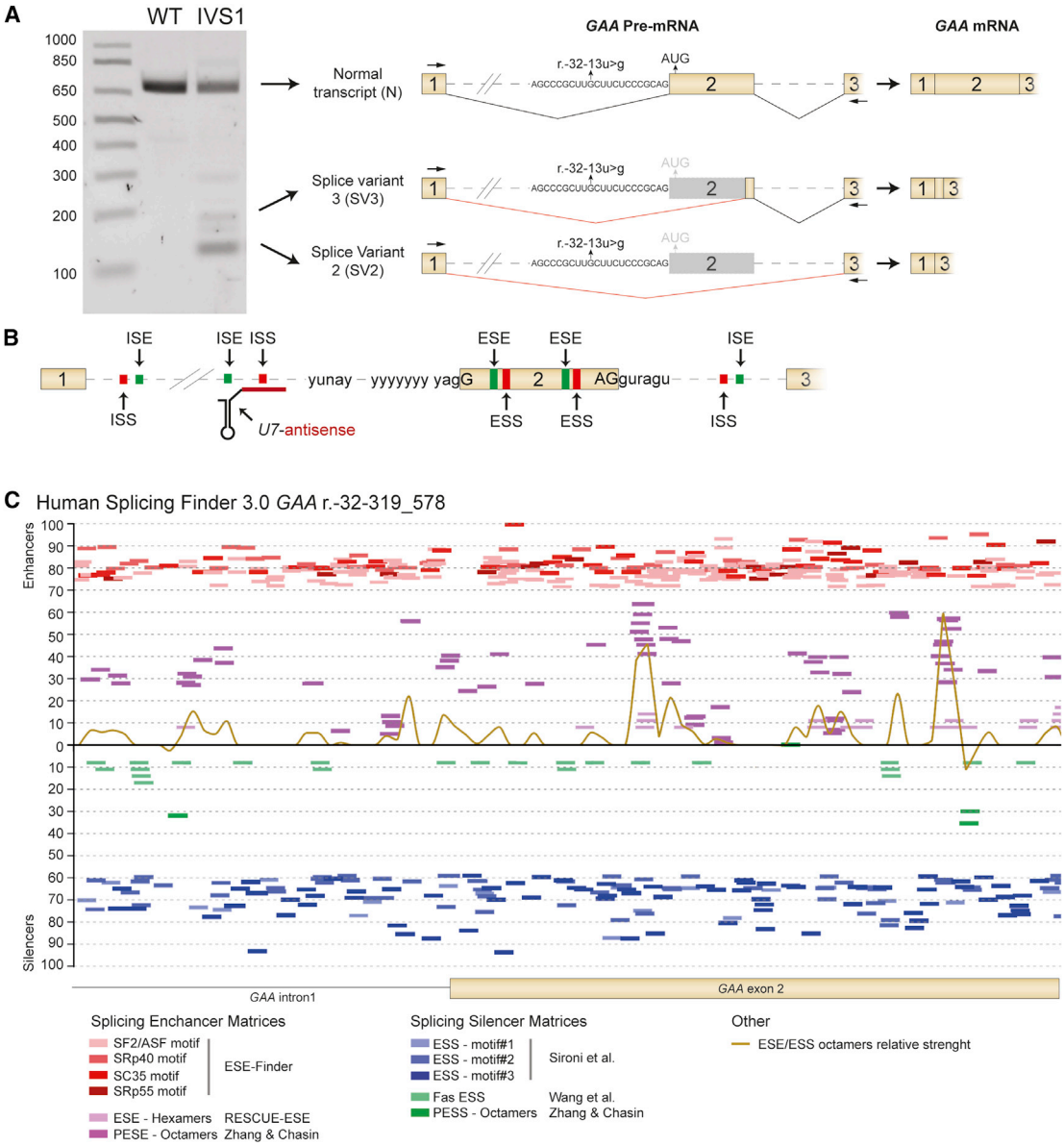

Figure 1. In Silico Prediction to Identify Splicing Regulatory Elements Surrounding the IVS1 Variant

(A) Outline of the three major splicing products of the *GAA* pre-mRNA caused by the IVS1 variant in a patient-derived primary fibroblast. The gel illustrates the results of flanking exon RT-PCR analysis of *GAA* exon 2 using primers that anneal to exon 1 and exon 3. Loading from left to right is as follows: DNA size markers (in basepairs); WT indicates control fibroblasts and IVS1 denotes fibroblasts from patient 1. Cartoons of pre-mRNAs illustrate splicing events as described.[24–27] The location of the r.-32-13u>g (IVS1) variant in the pY tract is indicated. Spliced mRNA cartoons are shown on the far right. (B) Cartoon showing hypothetical splicing regulatory elements that may be subject to modulation (e.g., by a *U7* snRNA). (C) In silico prediction in Human Splicing Finder 3.0 (http://www.umd.be/HSF3/) of exonic and intronic splicing silencers surrounding the *GAA* IVS1 variant. Algorithms used are indicated below the graph. PESE, putative exonic splicing enhancers; PESS, putative exonic splicing silencers.

that cover part of intron 1 and the complete exon 2 of the *GAA* pre-mRNA (Figure 2A). Because of the high costs involved when testing a large series of chemically modified AONs, AONs were expressed as *U7* snRNAs using a lentiviral vector. The original *U7* snRNA vector was adapted to enable one-step cloning of an AON and intermediate throughput screening (Figure S1A).[29] To validate the *U7* snRNA vector, a control experiment was performed on primary fibroblasts derived from a patient with adult Pompe disease (patient 1), who carried the IVS1 variant on one allele and the c.525delT on the second allele. A *U7* snRNA-based AON was targeted to the splice sites of exon 4 of *cyclophilin A* (*CypA*) pre-mRNA (Figure S1B). This AON was capable of inducing skipping of exon 4, as shown by flanking exon RT-PCR (Figure S1C) and exon internal qRT-PCR analysis (Figure S1D). This confirmed previous reports[29] and demonstrated

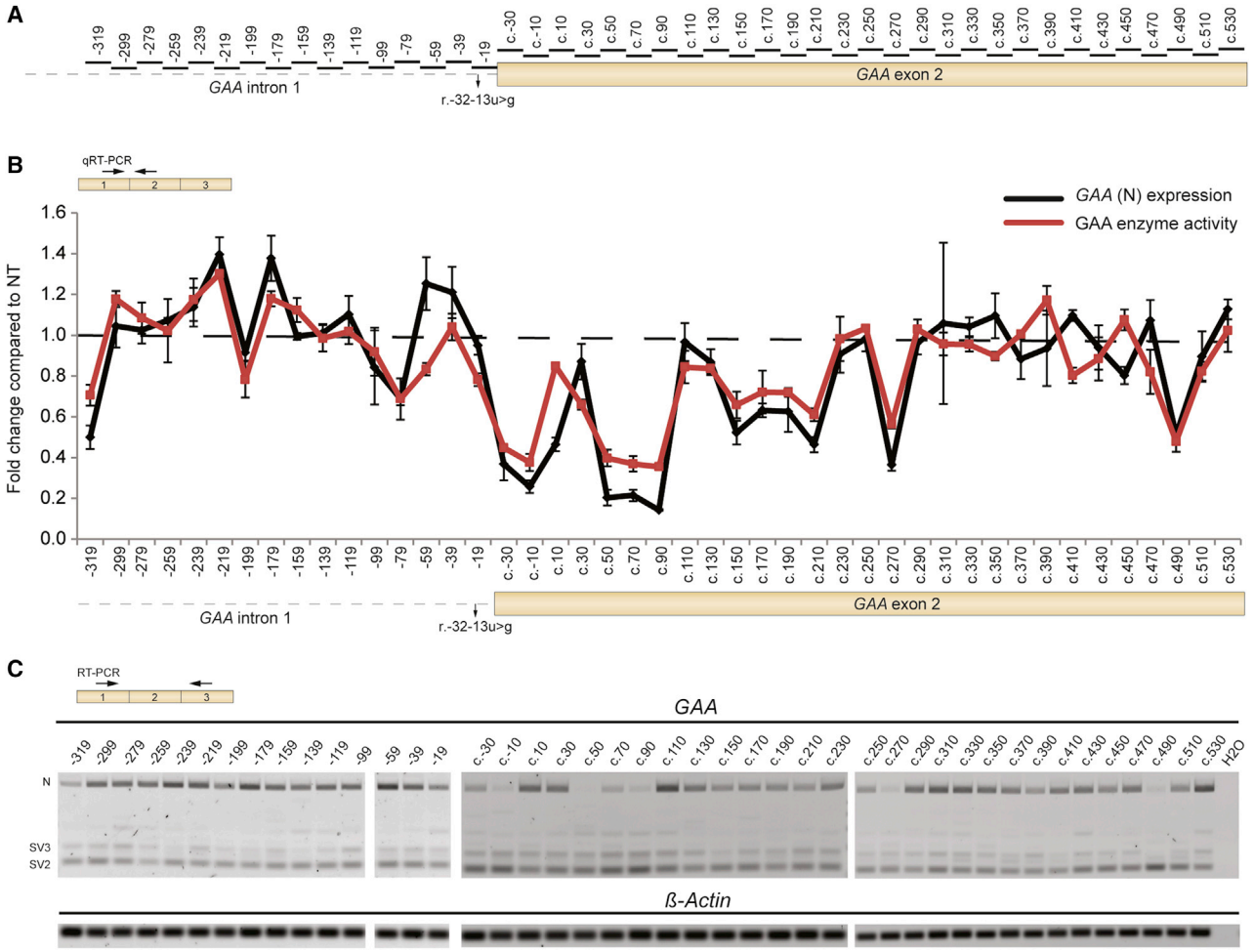

Figure 2. *U7* snRNA Screen to Identify Splicing Regulatory Elements Involved in *GAA* Exon 2 Splicing

(A) Locations of *U7* snRNA-based AONs generated for the screen in (B). (B) Screen to identify splicing regulatory elements that negatively regulate splicing of *GAA* exon 2. Primary fibroblasts from patient 1 (IVS1, c.525delT) were transduced with *U7* snRNA-expressing lentiviruses (200 ng p24 protein as determined by ELISA). The effects on *GAA* exon 2 expression were measured using qRT-PCR (black line; *GAA* [N] expression; primers are indicated in the upper left cartoon). Effects on GAA enzymatic activity are indicated by the red line. The cartoon of *GAA* pre-mRNA below the graph indicates the positions of the AONs tested. Data are expressed relative to non-transduced (NT) fibroblasts and represent means ± SD of three biological replicates. Samples were normalized for *β-Actin* expression. (C) The experiment in (B) was also analyzed by flanking exon RT-PCR of *GAA* exon 2. *β-Actin* mRNA was used as loading control. Primers are indicated in the upper left cartoon. (n = 3).

that the modified *U7* snRNA construct can be used to modulate splicing. Subsequently, the *U7* snRNA screen using the AONs indicated in Figure 2A was performed on fibroblasts from patient 1. The screen resulted in the identification of a number of *U7* snRNA-based AONs that modulated inclusion of exon 2 in the *GAA* mRNA, as shown with qRT-PCR analysis (Figure 2B, black line). Importantly, only mRNA from the allele carrying the IVS1 variant was detected due to the frameshift induced by the c.525delT variant on the second allele, which results in mRNA degradation. Notably, *U7* snRNAs targeting two regions in intron 1, at c.-32-179 and c.-32-219, promoted inclusion of *GAA* exon 2. Exclusion of exon 2 was promoted by *U7* snRNAs that targeted regions in the 5′ part of exon 2. Similar results were obtained using flanking exon RT-PCR analysis (Figure 2C). Promotion and inhibition of exon 2 inclusion resulted in increased and decreased GAA enzymatic activity, respectively (Figure 2B, compare black and red lines).

Next, the effect of the lentiviral amount was tested using p24 ELISA; 200 ng yielded an optimal ratio between biological effect and nonspecific reduction of cell viability and *GAA* expression seen at high viral amounts (Figure S2). To fine-tune the optimal location of *U7* snRNAs targeting c.-32-179 and c.-32-219, a microwalk was performed around these regions with *U7* snRNAs that shifted 2 nt (Figure 3A). This showed that the locations identified using the initial *U7* snRNA screen were peak values. In addition, the microwalk revealed two nearby locations at c.-32-183 and c.-32-185 whose inhibition promoted exon 2 inclusion (Figures 3B and 3C). Taken together, the *U7*-based snRNA screen of intron 1 and

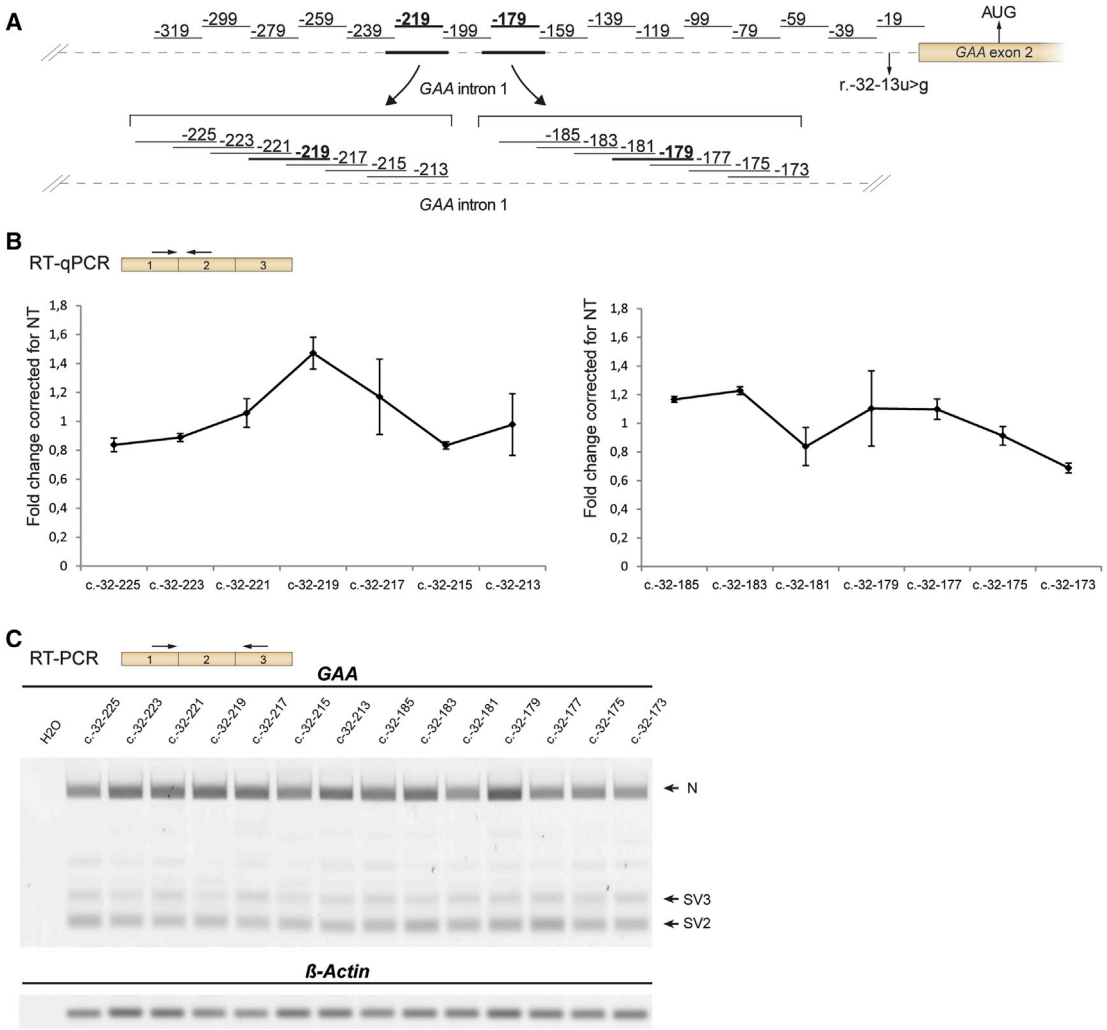

Figure 3. *U7* snRNA-Based Miniscreen of Targets Identified with the Large Screen

(A) Two hits from the screen shown in Figures 2B and 2C (in bold) were further tested in a microwalk using the *U7* snRNA system. Primer locations are indicated in the cartoon. (B) Results of the microwalk, as analyzed by qRT-PCR. (C) As in (B), using RT-PCR analysis. Results are expressed relative to non-transduced fibroblasts and represent means ± SD of three biological replicates.

exon 2 identified regions potentially involved in repression of *GAA* exon 2 inclusion.

Blockage of Splicing Repressor Sequences Using Antisense Oligonucleotides

To test whether morpholino-based AONs can modulate aberrant splicing caused by the IVS1 variant, AONs were designed based on the results from the *U7* snRNA screen shown in Figure 3. Specific requirements of low G content on chemical synthesis posed constrains to the regions that could be targeted but it was possible to design AONs that targeted the two major putative repressor sequences at c.-32-219 (AONs 1 and 2) and c.-32-179 (AONs 3 and 4) (Figures 4A and S3A). To test whether primary fibroblasts were amenable to splicing modulation using morpholino-based AONs, AONs targeting *CypA* were used as positive control. Two PMO-based AONs that target the 3′ donor splice site of exon 4 in the *CypA* pre-mRNA (Figures S3A and S3B) were able to promote skipping of exon 4 and exons 3 and 4 after transfection into primary fibroblasts, as shown by flanking exon RT-PCR and qRT-PCR analysis (Figures S3C and S3D), which is in agreement with our previous report.[9] Next, AONs 1–4 targeting the identified regions in the *GAA* pre-mRNA were tested by transfecting primary fibroblasts from patient 1. qRT-PCR analysis of exon 2 inclusion showed that AONs 3 and 4 promoted exon 2 inclusion more than 2-fold, whereas AONs 1 and 2 were ineffective (Figure 4B). Concomitant effects on GAA enzymatic activity were found, with more than 2-fold enhancement by AONs 3 and 4, while AONs 1 and 2 had no effect. This showed that PMO-based AONs that targeted the region of c.-32-179 promoted exon 2 inclusion, and that other PMO-based AONs tested were ineffective.

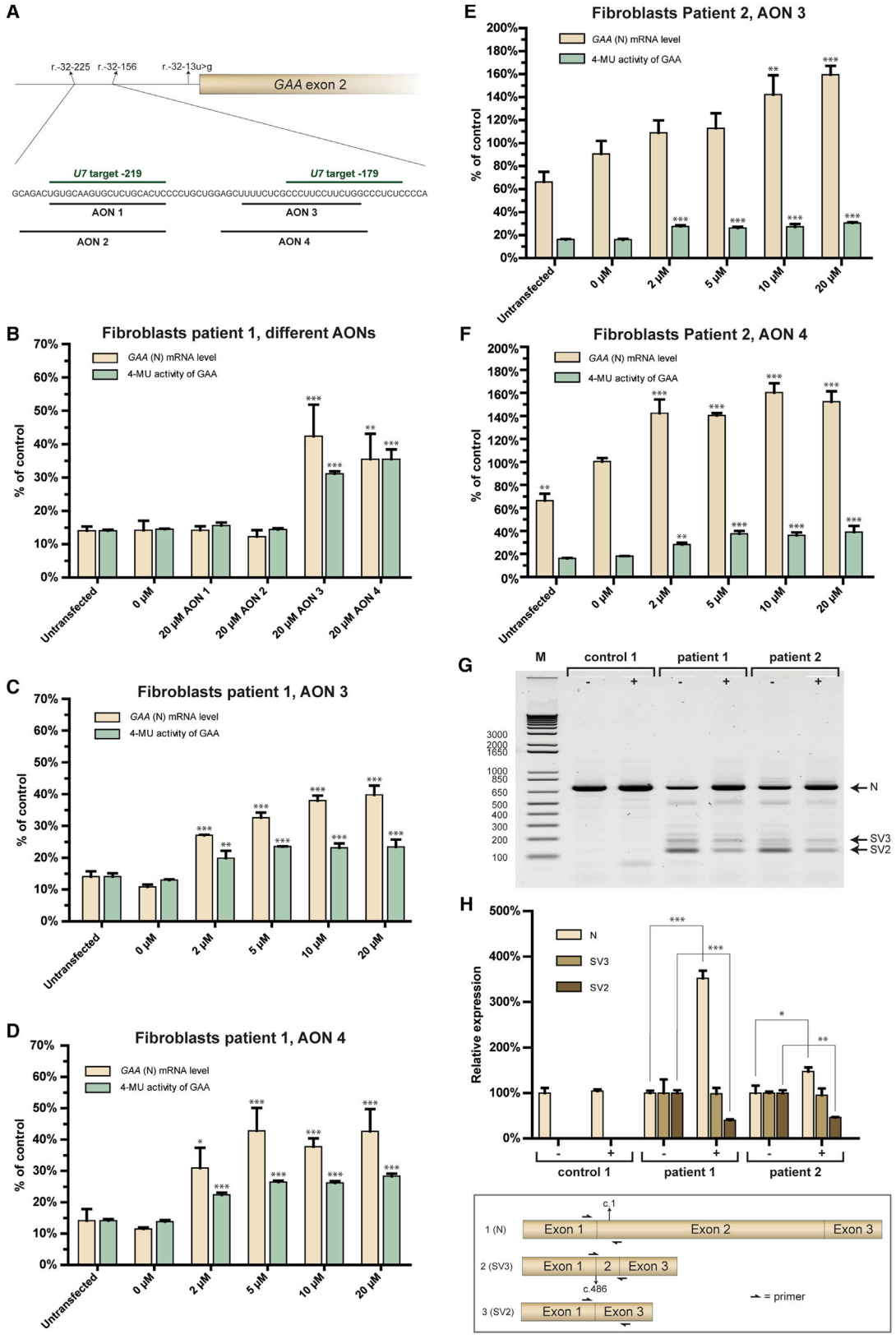

(legend on next page)

Next, the concentration-dependent effects of AONs 3 and 4 were tested after transfection in fibroblasts from patient 1 (Figures 4C and 4D). AONs 3 and 4 induced a concentration-dependent increase in both the expression of full-length *GAA* transcript and GAA enzymatic activity. Effects were almost maximal at 2 μM AON and reached a maximum at 5–20 μM. These results were confirmed in a fibroblast cell line from patient 2 (Figures 4E and 4F). This patient (genotype IVS1/c.923A>C) contained a missense *GAA* variant on allele 2, which was expressed at the mRNA level and led to a high "background" *GAA* cDNA level in the RT-PCR assays. We conclude that AONs 3 and 4 show in vitro activities that are sufficient to elevate canonical *GAA* pre-mRNA splicing, and thus GAA enzymatic activity, to above the disease threshold of 20% of the average level present in healthy controls that has been established in the diagnostic department of our center.

To confirm the mechanism by which AON 3 and 4 enhanced GAA enzymatic activity (i.e., by modulating splicing rather than total gene expression), analysis of individual splicing products was performed. Of note, full-skip (SV2) and cryptic splicing transcripts (SV3) lack the translation start codon and are subject to mRNA degradation, hampering accurate relative quantification. The effect of AON 4 was tested in control fibroblasts and in fibroblast from patients 1 and 2. Semiquantitative RT-PCR analysis using primers annealing to exon 1 and exon 3 showed that in patients with IVS1, AON 4 treatment caused an increase in the amount of the full-length (N) transcript, while the amount of the full-skip (SV2) transcript was reduced (Figure 4G). The amount of cryptic splicing transcript SV3 remained unchanged. AON 4 had no effect on *GAA* expression in control cells. Quantitative analysis by qRT-PCR utilized splicing product-specific primers,[27] and this confirmed the semiquantitative analysis (Figure 4H). These results suggest that AON 4 enhances expression of wild-type *GAA* mRNA by promoting exon 2 inclusion during aberrant splicing caused by the IVS1 variant, rather than acting on enhancing total *GAA* gene expression. This is further supported by the lack of effect on *GAA* expression in control cells.

DISCUSSION

The purpose of this work was to test whether aberrant *GAA* splicing caused by the common IVS1 variant could be restored using AONs. To this end, we performed a lentiviral *U7* snRNA-based screen with the aim to identify splicing regulatory sequences that could be blocked to promote exon inclusion. Hits from this screen were tested using PMO-based AONs. Two AONs were identified that promoted exon inclusion and GAA enzyme activity to above the disease threshold of 20% of average healthy control levels. These results identify splicing regulatory elements that negatively regulate the IVS1 variant, and they provide proof of concept for the restoration of canonical splicing in cells from patients with Pompe disease.

The IVS1 *GAA* variant represented a challenging case, because it is located in the pY tract of exon 2 and weakens the recognition of the splice acceptor site of exon 2. It was not obvious whether it was possible to enhance exon inclusion using AONs, as no negative splice regulatory elements in the *GAA* gene have been described that could be amenable to inhibition using an AON. This contrasts with other, more rare, *GAA* variants that affect splicing by causing a major shift from canonical toward cryptic splicing. In these cases, AONs that prevent cryptic splicing could restore canonical splicing.[9] We were encouraged by the observation that the IVS1 variant also allows a low level of leaky wild-type splicing, indicating that canonical splicing was still possible and that the pY tract was still partially functional. Previous findings that small drugs could enhance exon 2 splicing strengthen this hypothesis.[26] We identified a splicing regulatory element in intron 1 that was located approximately 280 nt upstream of the canonical splice acceptor of *GAA* exon 2. In an accompanying work,[30] we show that this does not concern a classical ISS motif, but that it is the pY tract of a cryptic splice acceptor site that, together with a downstream splice donor, forms a pseudo exon.

Current prediction programs for the identification of *cis*-acting elements that modulate splicing outcome vary widely in outcome, as illustrated in Figure 1C. We therefore performed an unbiased screen using *U7* snRNA-based AONs modified from Liu et al.[16,29] The lentiviral vector employed here was modified to enable one-step cloning with a >90% success rate. Lentiviral transduction showed near 100% infection of target cells, ensuring expression of the *U7* snRNAs in all target cells (data not shown). An alternative approach would be to order all desired AONs and to transfect directly in target cells, but this is expensive and not feasible for most research laboratories. The *U7* snRNA-based approach identified splicing regulatory motifs

Figure 4. Splicing Correction of *GAA* Exon 2 Using PMO-Based AONs

(A) Positions in the *GAA* pre-mRNA to which PMO-based AONs1–4 anneal. (B) Effect of AONs1–4 in fibroblasts from patient 1. *GAA* exon 2 inclusion in the mRNA was measured using qRT-PCR analysis (*GAA* [N] mRNA level) and GAA enzymatic activity using 4-methylumbelliferylα-D-glucopyranoside (4-MU) as substrate. Data are expressed relative to the average levels in healthy control fibroblasts and were corrected for *β-Actin* expression. (C) As in (B) but now using a concentration range of AON 3. (D) As in (B) but now using a concentration range of AON 4. (E) As in (C) but now with the treatment of patient 2 fibroblasts. (F) As in (D) but now with the treatment of patient 2 fibroblasts. (G) Flanking exon RT-PCR analysis of the effect of AON 4 on *GAA* exon 2 inclusion in fibroblasts from patient 1 and 2. −, 0 μM AON; +, 20 μM AON. (H) qRT-PCR analysis of individual splicing products of *GAA* exon 2 splicing. The N, SV2, and SV3 products were quantified using primers as outlined in the cartoon, and the effect of AON 4 on *GAA* exon 2 splicing was determined in fibroblasts from patients 1 and 2 and control 1. Data are corrected for *β-Actin* expression and normalized per splicing variant for expression in untreated cells to visualize the effect per variant. Note that patient 2 carried a pathogenic missense *GAA* variant on the second allele. *GAA* mRNA is normally expressed from this allele, which partially masks the effect on mRNA expression from the IVS1 allele. Patient 1 has no *GAA* mRNA expression from the second allele due to the presence of a variant that causes a frame shift and subsequent mRNA degradation. Data are means ± SDs of three biological replicates. *$p < 0.05$; **$p < 0.01$; ***$p < 0.001$.

that both reduce (intron 1) and enhance (5′ part of exon 2) inclusion of *GAA* exon 2 (Figure 2B). We were unable to identify these sequences using currently available splicing prediction programs,[31] highlighting the need for experimental work. This approach should be more generally applicable to unravel basic mechanisms of splicing and to identify therapeutic targets for splicing variants in human disease.

Metabolic disorders such as Pompe disease are good candidates for AON-mediated splicing correction. Often the enzyme deficiency only needs elevation to levels above a threshold to be fully functional.[32–34] Hits from the *U7* snRNA screen were tested using PMO-based AONs, and these promoted exon inclusion and GAA enzyme activity to above the disease threshold of 20%. This threshold was evident from the evaluation of fibroblast samples (using 4-MU as substrate) from ~700 individuals in our center, ~350 of which were diagnosed with Pompe disease based on clinical examination, muscle pathology, and biochemical and DNA analysis. While GAA enzyme activity levels in patients never exceeded 20%, the level in healthy individuals ranged from 40% to 180%. We note that the GAA enzyme activity assay is very sensitive to cell culture and assay conditions, and different patient and normal ranges (and therefore disease thresholds) may apply depending on the diagnostic center. Usually the IVS1 variant is present in combination with a variant on the second allele with no residual enzymatic activity, causing childhood/adult Pompe disease, although homozygosity of the IVS1 variant has been described in some patients with Pompe disease.[35,36] Full restoration of the IVS1 allele in compound heterozygous patients would provide a maximum of 50% GAA activity relative to the average levels in healthy controls, and this activity is within the range of healthy controls.

These results form a proof of concept for the development of a potential alternative treatment of a large percentage of Caucasian patients with Pompe disease. Current enzyme replacement therapy has limitations and is based on intravenous delivery of rhGAA that is taken up by target cells via mannose-6-phosphate receptor-mediated endocytosis. AON-mediated splicing correction presents a different strategy, as it enhances endogenous production of wild-type GAA enzyme. Further work is required to test the potential of the identified AONs for clinical implementation. The first step is to test AONs in the relevant cell type, skeletal muscle cells, as splicing can be cell-type specific.[37] This is described in our accompanying work.[30] Another aspect is cellular uptake by skeletal muscle in vivo following systemic delivery. AON treatments are well tolerated without serious adverse events, as shown in phase I and II clinical trials using 2′-O-methoxyethyl phosphorothioate and PMO chemistries for spinal muscular atrophy and Duchenne muscular dystrophy, respectively.[23,38] This may accelerate testing of AONs for the treatment of Pompe disease in a clinical setting. The ongoing development of improved methods for AON delivery, including tricyclo-DNA-based backbones[39] and cell-penetrating peptides like Pip6A,[40] is expected to be relevant for the future testing of AON-based drugs for the treatment of Pompe disease.

MATERIALS AND METHODS

Obtaining Patient Fibroblasts

Dermal fibroblasts from one control (control 1) and two patients (patients 1 and 2) with Pompe disease were obtained via skin biopsy with informed consent. The Erasmus Medical Center (MC) institutional review board approved the study protocol. All patient and control primary cell lines were negative for HIV, hepatitis B, and hepatitis C as tested by qPCR analysis at the diagnostic Department of Virology of the Erasmus MC Rotterdam. Both patient cell lines contain the IVS1 mutation on one allele. The second allele was c.525delT for patient 1 and c.923A>C (his>pro) for patient 2, which both are established pathogenic *GAA* variants (www.pompecenter.nl).

Nomenclature

Indications to variants and/or locations on the cDNA or (pre-)mRNA conform to Human Genome Variation Society (HGVS) standards (http://www.hgvs.org/mutnomen/).[41]

Modification of the U7 snRNA Vector for Efficient One-Step Cloning of AON Sequences

The *U7* snRNA gene and promoter were amplified by PCR from female mouse genomic DNA using Fw-ms-*U7* snRNA-Pst1 and rv-ms-*U7* snRNA-SalI primers, which included PstI and SalI overhang restriction sites. The PCR fragment (425 bp) was cloned into a pCRII-TOPO vector according to the manufacturer's manual (Invitrogen). SMopt and NsiI sites were generated by site-directed mutagenesis according to an inner and outer primer design with Fw- and Rv-*U7* snRNA-SMopt or Fw- and Rv-*U7* snRNA-NsiI as inner primers and with Fw-M13 and Rv-M13 as outer primers (Table S1), and they were subcloned using the PstI and SalI sites upstream of the polypurine tract fragment of the lentiviral vector used for reprogramming, from which OSKM and the spleen focus-forming virus (SF) promoter were removed.

Cloning of AONs into the U7 snRNA Vector

AONs were inserted via PCR amplification using a forward primer that contained the desired antisense sequence and the unique NsiI restriction site and the reverse primer Rv-ms- *U7* snRNA-SalI. The amplified PCR product was purified by agarose gel electrophoresis, extracted using the gel extraction kit (QIAGEN), digested with NsiI and SalI, purified with a PCR purification kit from (QIAGEN), and cloned into the NsiI and SalI sites of the *U7* snRNA vector. Clones were verified by sequencing with the Fw-ms-*U7* snRNA-PstI (Table S1) and restriction enzyme digestion.

Cell Culture

Both HEK293T cells and human primary fibroblasts were cultured in high-glucose DMEM (Gibco) supplemented with 100 U/mL penicillin/streptomycin/glutamine (Gibco/Thermo Scientific) and 10% fetal bovine serum (Hyclone/Thermo Scientific). Cells were passaged after reaching 80%/90% confluence with TrypLE (Gibco/Thermo Scientific). All cell lines were routinely tested for mycoplasma infection

using the MycoAlert Mycoplasma Detection Kit (Lonza) and were negative.

Virus Production

Lentiviruses were produced by co-transfecting HEK293T cells at 80% confluence in a 10-cm culture dish with the lentivirus transfer vector (3 μg SF-*U7* snRNA vectors) and packaging plasmids (2 μg psPAX2 and 1 μg pVSV vectors) using Fugene 6 transfection according to the manufacturer's protocol (Promega). Lentiviruses were harvested from the medium after 72 hr of transfection and were filtered using a 0.45-μm polyvinylidene fluoride (PVDF) filter (Millipore). After filtering, lentiviruses were concentrated by high-speed centrifugation for 2 hr at 20,000 rpm in a Beckman Coulter Ultracentrifuge with a SW32 Ti rotor at 4°C. The supernatant was removed and the pellet was resuspended in 25 μL low-glucose DMEM (Invitrogen) per plate. The virus was stored in aliquots at −80°C.

p24 ELISA

Viral titers were determined with the HIV-1 p24 antigen ELISA kit (Retrotek; Zeptomix) according to the manufacturer's manual. Each virus was diluted 1:400,000 and 1:1,000,000 and the optical density at 450 nm (OD_{450}) was measured with the Varioskan reader (Thermo Scientific).

Transduction of *U7* snRNA Vectors

One day before infection, 6×10^4 cells per single well of a 12-well plate of primary fibroblasts derived from patient 1 were seeded. One day later, the cells were infected with 200 ng virus containing the SF-*U7* snRNA constructs; after 24 hr, cells were washed three times with PBS before fresh medium was added. After 4 days, cells were washed with PBS and harvested with RLT buffer from the RNAeasy kit for RNA isolation (QIAGEN). For the GAA enzyme activity assay, cells were harvested after 12 days.

Morpholino Transfections

Fibroblasts were transfected with morpholino AONs using Endoporter reagent (Gene-Tools). Cells were grown to 90% confluence before transfection. Endoporter reagent was used at a concentration of 4.5 μL/mL medium. Morpholinos were dissolved in sterile water to a concentration of 1 mM and the appropriate volume was added to each culture well. Cells were harvested 3–5 days after AON addition.

RNA Isolation and cDNA Synthesis

RNA was extracted with the RNeasy Mini Kit with DNase treatment (QIAGEN) and was stored at −80°C in RNase-free water. cDNA was synthesized from 500 ng RNA using the iScript cDNA synthesis kit (Bio-Rad).

qRT-PCR

cDNA was diluted 5, 10, or 20 times and used with 7.5 μL iTaq Universal SYBR Green Supermix (Bio-Rad) with 10 pmol/μL forward and reverse primers (Table S1) in a CFX96 real-time system (Bio-Rad). Cycle threshold (Ct) values were related to amounts using standard curves of four to six dilutions. Quantification of expression was calculated relative to *β-Actin* expression.

Flanking Exon RT-PCR of *GAA*

cDNA (diluted 10 times) with GC *GAA* exon 1–3 fw and GC *GAA* exon 1–3 rv primers (Table S1) were used for RT-PCR with the Advantage GC 2 PCR kit (Clontech/Takara) and a GC-melt concentration of 0.5 M according to the manufacturer's protocol. The whole GC-PCR reaction was analyzed on a 1.5% agarose gel containing 0.5 μg/mL ethidium bromide (Sigma-Aldrich).

GAA Enzyme Activity Assay

Cells were harvested with ice-cold lysis buffer (50 mM Tris, pH 7.5, 100 mM NaCl, 50 mM NaF, 1% Triton X-100, and one tablet of Roche cOmplete Protease Inhibitor Cocktail, with EDTA) and incubated for 10 min on ice. Samples were centrifuged at 14,000 rpm for 10 min at 4°C. GAA enzyme activity was measured using 4-MU (Sigma-Aldrich) as substrate as described.[27] Total protein concentration was determined using a BCA protein assay kit (Pierce/Thermo Scientific).

Because GAA enzyme activity data strongly depend on assay conditions and so we could evaluate enzyme activities relative to the disease threshold, we normalized the data based on two criteria: (1) the enzyme activity of patient cells measured in a diagnostic setting rather than a research setting, and (2) the average enzyme activity present in healthy control fibroblasts. These results, expressed as the percent of control, are presented in Figure 4. Enzyme data without normalization are shown in Figure S4.

Statistical Analysis

All data represent means ± SD, and p values refer to two-sided Student's t tests. The Bonferroni multiple testing correction was applied where necessary. A p value < 0.05 was considered significant. Data showed normal variance. There was no power calculation in any of the experiments. No randomization method was used. No samples were excluded from the analyses. Investigators were not blinded to the identity of the samples.

SUPPLEMENTAL INFORMATION

Supplemental Information includes four figures and one table and can be found with this article online at http://dx.doi.org/10.1016/j.omtn.2017.03.001.

AUTHOR CONTRIBUTIONS

E.v.d.W., A.J.B., A.T.v.d.P., and W.W.M.P.P. conceived and designed the study and drafted the manuscript. E.v.d.W., A.J.B., and J.M.P. performed the experiments. W.W.M.P.P supervised the study. E.v.d.W., A.J.B., J.M.P., A.T.v.d.P., and W.W.M.P.P. were involved in data interpretation and approved the final manuscript.

CONFLICTS OF INTEREST

A.T.v.d.P. has provided consulting services for various industries in the field of Pompe disease under an agreement between these

industries and Erasmus MC. The other authors declare no conflicts of interest.

ACKNOWLEDGMENTS

We thank Philip Lijnzaad for advice on statistical analysis and Dr. Arnold Reuser for discussion. This work was funded by grants from the Sophia Children's Hospital Foundation (SSWO) (S-687) and the Prinses Beatrix Spierfonds/Stichting Spieren voor Spieren (W.OR13-21).

REFERENCES

1. Chen, L., Bush, S.J., Tovar-Corona, J.M., Castillo-Morales, A., and Urrutia, A.O. (2014). Correcting for differential transcript coverage reveals a strong relationship between alternative splicing and organism complexity. Mol. Biol. Evol. *31*, 1402–1413.
2. Lee, Y., and Rio, D.C. (2015). Mechanisms and regulation of alternative pre-mRNA splicing. Annu. Rev. Biochem. *84*, 291–323.
3. Jangi, M., and Sharp, P.A. (2014). Building robust transcriptomes with master splicing factors. Cell *159*, 487–498.
4. Moehle, E.A., Braberg, H., Krogan, N.J., and Guthrie, C. (2014). Adventures in time and space: splicing efficiency and RNA polymerase II elongation rate. RNA Biol. *11*, 313–319.
5. Jonkers, I., and Lis, J.T. (2015). Getting up to speed with transcription elongation by RNA polymerase II. Nat. Rev. Mol. Cell Biol. *16*, 167–177.
6. Movassat, M., Crabb, T.L., Busch, A., Yao, C., Reynolds, D.J., Shi, Y., and Hertel, K.J. (2016). Coupling between alternative polyadenylation and alternative splicing is limited to terminal introns. RNA Biol. *13*, 646–655.
7. Naftelberg, S., Schor, I.E., Ast, G., and Kornblihtt, A.R. (2015). Regulation of alternative splicing through coupling with transcription and chromatin structure. Annu. Rev. Biochem. *84*, 165–198.
8. Krawczak, M., Thomas, N.S., Hundrieser, B., Mort, M., Wittig, M., Hampe, J., and Cooper, D.N. (2007). Single base-pair substitutions in exon-intron junctions of human genes: nature, distribution, and consequences for mRNA splicing. Hum. Mutat. *28*, 150–158.
9. Bergsma, A.J., In 't Groen, S.L., Verheijen, F.W., van der Ploeg, A.T., and Pijnappel, W.P. (2016). From cryptic toward canonical pre-mRNA splicing in Pompe disease: a pipeline for the development of antisense oligonucleotides. Mol. Ther. Nucleic Acids *5*, e361.
10. Weber, A., Kreth, J., and Müller, U. (2016). Intronic PRRT2 mutation generates novel splice acceptor site and causes paroxysmal kinesigenic dyskinesia with infantile convulsions (PKD/IC) in a three generation family. BMC Med. Genet. *17*, 16.
11. Stucki, M., Suormala, T., Fowler, B., Valle, D., and Baumgartner, M.R. (2009). Cryptic exon activation by disruption of exon splice enhancer: novel mechanism causing 3-methylcrotonyl-CoA carboxylase deficiency. J. Biol. Chem. *284*, 28953–28957.
12. Kashima, T., and Manley, J.L. (2003). A negative element in SMN2 exon 7 inhibits splicing in spinal muscular atrophy. Nat. Genet. *34*, 460–463.
13. Wang, E.T., Cody, N.A., Jog, S., Biancolella, M., Wang, T.T., Treacy, D.J., Luo, S., Schroth, G.P., Housman, D.E., Reddy, S., et al. (2012). Transcriptome-wide regulation of pre-mRNA splicing and mRNA localization by muscleblind proteins. Cell *150*, 710–724.
14. Yoshida, K., Sanada, M., Shiraishi, Y., Nowak, D., Nagata, Y., Yamamoto, R., Sato, Y., Sato-Otsubo, A., Kon, A., Nagasaki, M., et al. (2011). Frequent pathway mutations of splicing machinery in myelodysplasia. Nature *478*, 64–69.
15. Soldati, D., and Schümperli, D. (1988). Structural and functional characterization of mouse U7 small nuclear RNA active in 3′ processing of histone pre-mRNA. Mol. Cell. Biol. *8*, 1518–1524.
16. Gorman, L., Suter, D., Emerick, V., Schümperli, D., and Kole, R. (1998). Stable alteration of pre-mRNA splicing patterns by modified U7 small nuclear RNAs. Proc. Natl. Acad. Sci. USA *95*, 4929–4934.
17. Havens, M.A., and Hastings, M.L. (2016). Splice-switching antisense oligonucleotides as therapeutic drugs. Nucleic Acids Res. *44*, 6549–6563.
18. Buzin, C.H., Feng, J., Yan, J., Scaringe, W., Liu, Q., den Dunnen, J., Mendell, J.R., and Sommer, S.S. (2005). Mutation rates in the dystrophin gene: a hotspot of mutation at a CpG dinucleotide. Hum. Mutat. *25*, 177–188.
19. Flanigan, K.M., Dunn, D.M., von Niederhausern, A., Soltanzadeh, P., Gappmaier, E., Howard, M.T., Sampson, J.B., Mendell, J.R., Wall, C., King, W.M., et al.; United Dystrophinopathy Project Consortium (2009). Mutational spectrum of DMD mutations in dystrophinopathy patients: application of modern diagnostic techniques to a large cohort. Hum. Mutat. *30*, 1657–1666.
20. Traynor, K. (2016). Eteplirsen approved for Duchenne muscular dystrophy. Am. J. Health Syst. Pharm. *73*, 1719.
21. Hua, Y., Vickers, T.A., Okunola, H.L., Bennett, C.F., and Krainer, A.R. (2008). Antisense masking of an hnRNP A1/A2 intronic splicing silencer corrects SMN2 splicing in transgenic mice. Am. J. Hum. Genet. *82*, 834–848.
22. Hua, Y., Vickers, T.A., Baker, B.F., Bennett, C.F., and Krainer, A.R. (2007). Enhancement of SMN2 exon 7 inclusion by antisense oligonucleotides targeting the exon. PLoS Biol. *5*, e73.
23. Haché, M., Swoboda, K.J., Sethna, N., Farrow-Gillespie, A., Khandji, A., Xia, S., and Bishop, K.M. (2016). Intrathecal injections in children with spinal muscular atrophy: nusinersen clinical trial experience. J. Child Neurol. *31*, 899–906.
24. Huie, M.L., Chen, A.S., Tsujino, S., Shanske, S., DiMauro, S., Engel, A.G., and Hirschhorn, R. (1994). Aberrant splicing in adult onset glycogen storage disease type II (GSDII): molecular identification of an IVS1 (-13T–>G) mutation in a majority of patients and a novel IVS10 (+1GT–>CT) mutation. Hum. Mol. Genet. *3*, 2231–2236.
25. Boerkoel, C.F., Exelbert, R., Nicastri, C., Nichols, R.C., Miller, F.W., Plotz, P.H., and Raben, N. (1995). Leaky splicing mutation in the acid maltase gene is associated with delayed onset of glycogenosis type II. Am. J. Hum. Genet. *56*, 887–897.
26. Dardis, A., Zanin, I., Zampieri, S., Stuani, C., Pianta, A., Romanello, M., Baralle, F.E., Bembi, B., and Buratti, E. (2014). Functional characterization of the common c.-32-13T>G mutation of GAA gene: identification of potential therapeutic agents. Nucleic Acids Res. *42*, 1291–1302.
27. Bergsma, A.J., Kroos, M., Hoogeveen-Westerveld, M., Halley, D., van der Ploeg, A.T., and Pijnappel, W.W. (2015). Identification and characterization of aberrant GAA pre-mRNA splicing in Pompe disease using a generic approach. Hum. Mutat. *36*, 57–68.
28. Kroos, M.A., Pomponio, R.J., Hagemans, M.L., Keulemans, J.L., Phipps, M., DeRiso, M., Palmer, R.E., Ausems, M.G., Van der Beek, N.A., Van Diggelen, O.P., et al. (2007). Broad spectrum of Pompe disease in patients with the same c.-32-13T->G haplotype. Neurology *68*, 110–115.
29. Liu, S., Asparuhova, M., Brondani, V., Ziekau, I., Klimkait, T., and Schümperli, D. (2004). Inhibition of HIV-1 multiplication by antisense U7 snRNAs and siRNAs targeting cyclophilin A. Nucleic Acids Res. *32*, 3752–3759.
30. Van der Wal, E., Bergsma, A.J., Van Gestel, T.J.G., In 't Groen, S.L.M., Zaehres, H., Araúzo-Bravo, M.J., Scholer, H.R., van der Ploeg, A.T., and Pijnappel, W.W.M.P. (2017). GAA deficiency in Pompe disease is alleviated by exon inclusion in iPS-derived skeletal muscle cells. Mol. Ther. Nucleic Acids. *7*, this issue, 101–115.
31. Desmet, F.O., Hamroun, D., Lalande, M., Collod-Béroud, G., Claustres, M., and Béroud, C. (2009). Human Splicing Finder: an online bioinformatics tool to predict splicing signals. Nucleic Acids Res. *37*, e67.
32. Altarescu, G.M., Goldfarb, L.G., Park, K.Y., Kaneski, C., Jeffries, N., Litvak, S., Nagle, J.W., and Schiffmann, R. (2001). Identification of fifteen novel mutations and genotype-phenotype relationship in Fabry disease. Clin. Genet. *60*, 46–51.
33. Huemer, M., Mulder-Bleile, R., Burda, P., Froese, D.S., Suormala, T., Zeev, B.B., Chinnery, P.F., Dionisi-Vici, C., Dobbelaere, D., Gökcay, G., et al. (2016). Clinical pattern, mutations and in vitro residual activity in 33 patients with severe 5, 10 methylenetetrahydrofolate reductase (MTHFR) deficiency. J. Inherit. Metab. Dis. *39*, 115–124.
34. Zhang, M., Liu, Y., Sun, S., Zhang, H., Wang, W., Ning, G., and Li, X. (2013). A prevalent and three novel mutations in CYP11B1 gene identified in Chinese patients with 11-beta hydroxylase deficiency. J. Steroid Biochem. Mol. Biol. *133*, 25–29.
35. Musumeci, O., Thieme, A., Claeys, K.G., Wenninger, S., Kley, R.A., Kuhn, M., Lukacs, Z., Deschauer, M., Gaeta, M., Toscano, A., et al. (2015). Homozygosity for the

common GAA gene splice site mutation c.-32-13T>G in Pompe disease is associated with the classical adult phenotypical spectrum. Neuromuscul. Disord. *25*, 719–724.

36. Laforêt, P., Nicolino, M., Eymard, P.B., Puech, J.P., Caillaud, C., Poenaru, L., and Fardeau, M. (2000). Juvenile and adult-onset acid maltase deficiency in France: genotype-phenotype correlation. Neurology *55*, 1122–1128.

37. Yeo, G., Holste, D., Kreiman, G., and Burge, C.B. (2004). Variation in alternative splicing across human tissues. Genome Biol. *5*, R74.

38. Mendell, J.R., Goemans, N., Lowes, L.P., Alfano, L.N., Berry, K., Shao, J., Kaye, E.M., and Mercuri, E.; Eteplirsen Study Group and Telethon Foundation DMD Italian Network (2016). Longitudinal effect of eteplirsen versus historical control on ambulation in Duchenne muscular dystrophy. Ann. Neurol. *79*, 257–271.

39. Goyenvalle, A., Griffith, G., Babbs, A., El Andaloussi, S., Ezzat, K., Avril, A., Dugovic, B., Chaussenot, R., Ferry, A., Voit, T., et al. (2015). Functional correction in mouse models of muscular dystrophy using exon-skipping tricyclo-DNA oligomers. Nat. Med. *21*, 270–275.

40. Godfrey, C., Muses, S., McClorey, G., Wells, K.E., Coursindel, T., Terry, R.L., Betts, C., Hammond, S., O'Donovan, L., Hildyard, J., et al. (2015). How much dystrophin is enough: the physiological consequences of different levels of dystrophin in the mdx mouse. Hum. Mol. Genet. *24*, 4225–4237.

41. den Dunnen, J.T., Dalgleish, R., Maglott, D.R., Hart, R.K., Greenblatt, M.S., McGowan-Jordan, J., Roux, A.F., Smith, T., Antonarakis, S.E., and Taschner, P.E. (2016). HGVS recommendations for the description of sequence variants: 2016 update. Hum. Mutat. *37*, 564–569.

OMTN, Volume *7*

Supplemental Information

Antisense Oligonucleotides Promote Exon Inclusion and Correct the Common c.-32-13T>G *GAA* Splicing Variant in Pompe Disease

Erik van der Wal, Atze J. Bergsma, Joon M. Pijnenburg, Ans T. van der Ploeg, and W.W.M. Pim Pijnappel

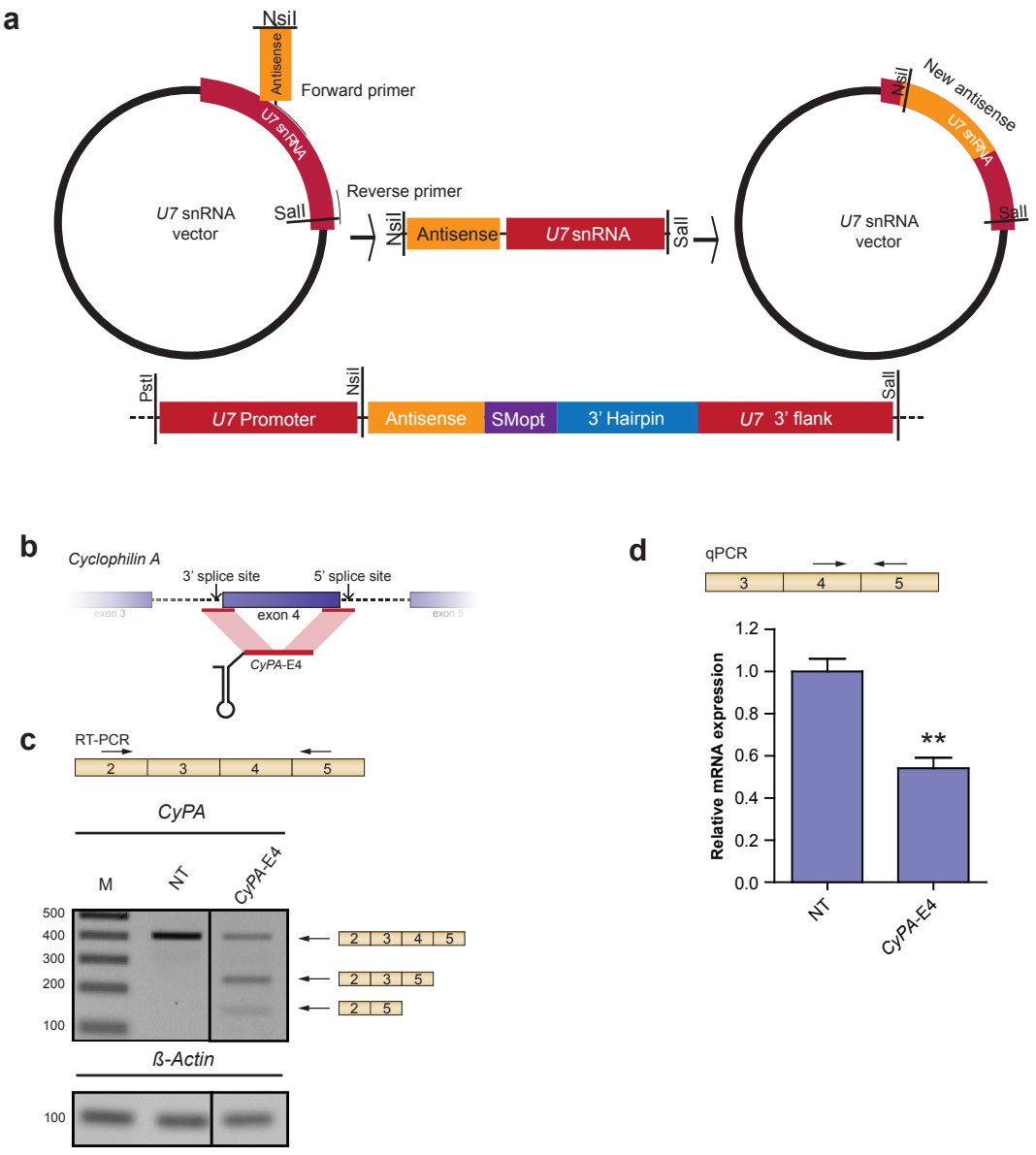

Figure S1. One step *U7* snRNA cloning system and validation. (a) One-step cloning strategy for rapid cloning of AONs in the lentiviral *U7* snRNA expression vector. A unique NsiI site was introduced in the *U7* snRNA. AON sequenc-es and the NsiI site were part of a forward primer in PCR, and a unique SalI site was included in the reverse PCR primer. **(b)** Cartoon of the region of the *Cyclophilin A* (*CypA*) gene that was targeted using a *U7* snRNA-expressed AON (*CyPA*-E4) as described previously by Liu et al.[1] **(c)** RT-PCR analysis of patient 1 fibroblasts in which the *CypA* pre-mRNA was targeted using *CyPA*-E4. As control, non-transduced cells were used (NT). The PCR strategy is shown above the gel. ß-Actin was used as loading control. **(d)** RT-qPCR analysis of the samples of **(c)**.

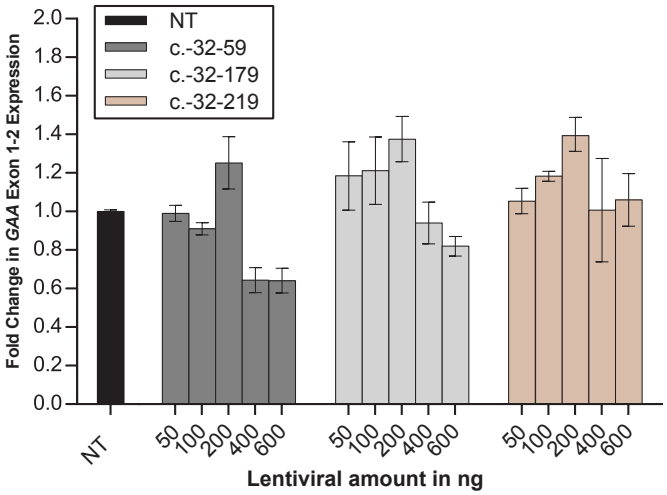

Figure S2. Testing of the optimal viral amount for detection of splicing modulation sequences. Patient 1 fibroblasts were infected with various lentiviruses at the amounts indicated. The optimum amount was determined to be 200 ng lentivirus per ml of medium. Data are means +/- SD of two biological replicates. Data points from 200 ng were taken from Figure 2B (N = 3). NT: non-transduced.

a

Name:	cDNA location	sequence 5' to 3'	nucleotides
CypA 1	*CypA* c.165_173+11	TGTACCCTTACCACTCAGTC	20
CypA 2	*CyPA* c.165_173+16	CATGTTGTACCCTTACCACTCAGTC	25
AON 1	*GAA* c.-32-219_-200	GAGTGCAGAGCACTTGCACA	20
AON 2	*GAA* c.-32-224_-200	GAGTGCAGAGCACTTGCACAGTCTG	25
AON 3	*GAA* c.-32-187_-167	CCAGAAGGAAGGGCGAGAAAA	21
AON 4	*GAA* c.-32-190_-166	GCCAGAAGGAAGGGCGAGAAAAGCT	25

reference sequence for cDNA annotation is NM_000152.3

b

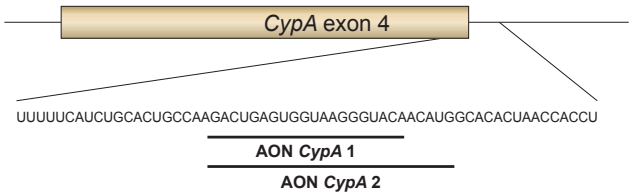

c

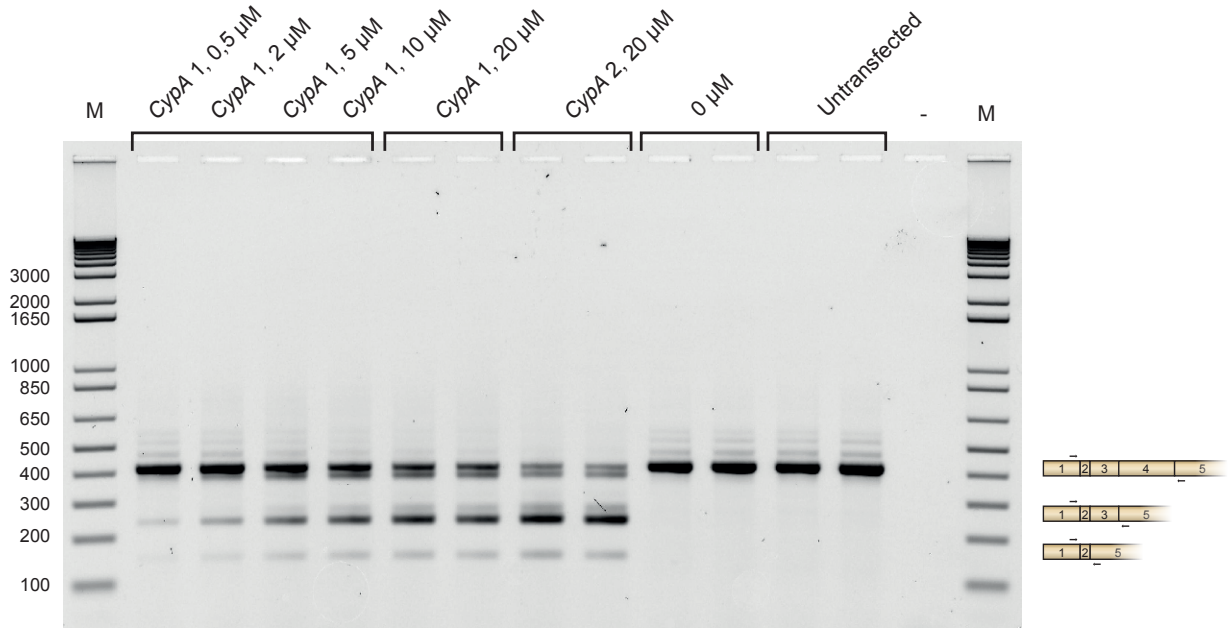

d

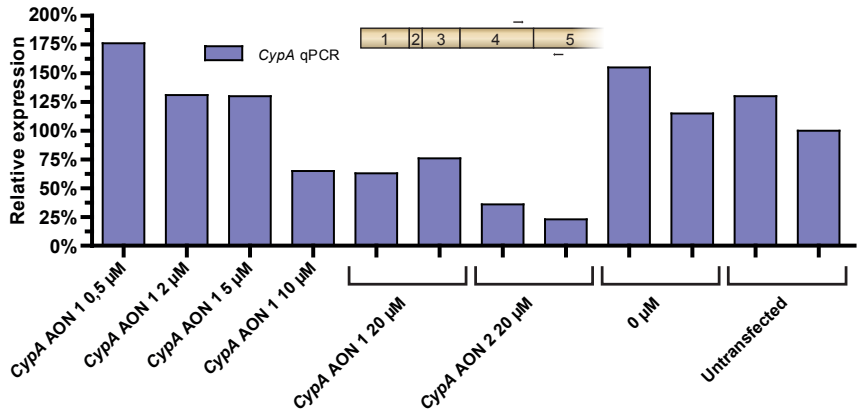

Figure S3. Validation of PMO-based AONs in primary fibroblasts. (a) Sequences of PMO-AONs used. **(b-d)** Test of PMO-based AONs on the positive control gene *CypA*. **(b)** Location of AONs designed to block the splice donor of *CypA* exon 4. **(c)** Fibroblasts from patient 1 were transfected with AONs at various concentrations as indicated, and *CyPA* mRNAs were analyzed by RT-PCR. Cartoons at the right side of the gel indicate spliced products. **(d)** RT-qPCR analysis of exon 4 skipping of the experiment in **(c)**. The cartoon highlights the primer locations. Data represent means of 3 technical replicates.

Table S1. Primers used for RT-qPCR, RT-PCR, cloning and sequencing

Primer target	Sequence (5'-3')	Used for
β-Actin fw	AACCGCGAGAAGATGACCC	qPCR/RT-PCR
β-Actin rv	GCCAGAGGCGTACAGGGATAG	qPCR/RT-PCR
GAA Exon 1-2 fw	AAACTGAGGCACGGAGCG	qPCR
GAA Exon 1-2 rv	GAGTGCAGCGGTTGCCAA	qPCR
GAA Cryptic Exon 2 fw	GGCACGGAGCGGGACA	qPCR
GAA Cryptic Exon 2 rv	CTGTTAGCTGGATCTTTGATCGTG	qPCR
GAA Full Skip Exon 2 fw	AGGCACGGAGCGGATCA	qPCR
GAA Full Skip Exon 2 rv	TCGGAGAACTCCACGCTGTA	qPCR
GAA Pseudo Exon fw	AAACTGAGGCACGGAGCG	qPCR
GAA Pseudo Exon rv	GCAGCTCTGAGACATCAACCG	qPCR
CypA Exon 2-5 fw	CACCGTGTTCTTCGACATTG	RT-PCR
CypA Exon 2-5 rv	CCATGGCCTCCACAATATTC	RT-PCR
CypA Exon 4-5 fw	GGACCCAACACAAATGGTTC	qPCR
CypA Exon 4-5 rv	GGCCTCCACAATATTCATGC	qPCR
Fw-*U7*snRNA-smOPT	GCTCTTTTAGAATTTTTGGAGCAGGTTTTCTGACTTCG	Cloning
Rv-*U7*snRNA-smOPT	CGAAGTCAGAAAACCTGCTCCAAAAATTCTAAAAGAGC	Cloning
Fw-*U7*snRNA-NsiI	CCTGGCTCGCTACAGATGCATAGGAGGACGGAGGACG	Cloning
Rv-*U7*snRNA-NsiI	CGTCCTCCGTCCTCCTATGCATCTGTAGCGAGCCAGG	Cloning
Fw-*U7*snRNA-PstI	GCGCCTGCAGTAACAACATAGGAGCTGTG	Cloning
Rv-*U7*snRNA-SalI	GCGCGTCGACCAGATACGCGTTTCCTAGGA	Cloning
M13 fw	GTAAAACGACGGGCCAG	Sequencing
M13 rv	CAGGAAACAGCTATGAC	Sequencing
GAA Exon1-3 fw	AGGTTCTCCTCGTCCGCCCGTTGTTCA	RT-PCR
GAA Exon1-3 rv	TCCAAGGGCACCTCGTAGCGCCTGTTA	RT-PCR

Supplemental References

1. Liu, S, Asparuhova, M, Brondani, V, Ziekau, I, Klimkait, T, and Schumperli, D (2004). Inhibition of HIV-1 multiplication by antisense U7 snRNAs and siRNAs targeting cyclophilin A. *Nucleic Acids Res* **32**: 3752-3759.